Published in final edited form as:
Cardiovasc Toxicol. 2013 December ; 13(4): . doi:10.1007/s12012-013-9215-1.

Protection from oxidative and electrophilic stress in the *Gsta4*-null mouse heart

Helen Beneš[1], **Mai K. Vuong**[1], **Marjan Boerma**[2], **Kevin E. McElhanon**[3], **Eric R. Siegel**[4], and **Sharda P. Singh**[3,5]

[1]Department of Neurobiology and Developmental Sciences, University of Arkansas for edical Sciences, Little Rock, Arkansas 72205, USA

[2]Department of Pharmaceutical Sciences, University of Arkansas for Medical Sciences, Little Rock, AR 72205, U.S.A

[3]Department of Pharmacology and Toxicology, University of Arkansas for Medical Sciences, Little Rock, AR 72205, U.S.A

[4]Department of Biostatistics, University of Arkansas for Medical Sciences, Little Rock, Arkansas 72205, USA

[5]Central Arkansas Veterans Healthcare System, Little Rock, AR 72205, U.S.A

Abstract

4-hydroxynonenal (4-HNE) mediates many pathological effects of oxidative and electrophilic stress and signals to activate cytoprotective gene expression regulated by NF-E2-related factor 2 (Nrf2). By exhibiting very high levels of 4-HNE-conjugating activity, the murine glutathione transferase alpha 4 (GSTA4-4) helps regulate cellular 4-HNE levels. To examine the role of 4-HNE *in vivo*, we disrupted the murine *Gsta4* gene. *Gsta4*-null mice exhibited no cardiac phenotype under normal conditions and no difference in cardiac 4-HNE level as compared to wild-type (WT) mice. We hypothesized that the Nrf2 pathway might contribute an important compensatory mechanism to remove excess cardiac 4-HNE in *Gsta4*-null mice. Cardiac nuclear extracts from *Gsta4*-null mice exhibited significantly higher Nrf2 binding to antioxidant-response elements (AREs). We also observed responses in critical Nrf2 target gene products: elevated *Sod2*, *Cat*, and *Akr1b7* mRNA levels and significant increases in both cardiac anti-oxidant and anti-electrophile enzyme activities. *Gsta4*-null mice were less sensitive and maintained normal cardiac function following chronic doxorubicin (DOX) treatment, known to increase cardiac 4-HNE levels. Hence, in the absence of GSTA4-4 to modulate both physiological and pathological 4-HNE levels, the adaptive Nrf2 pathway may be primed to contribute to a preconditioned cardiac phenotype in the *Gsta4*-null mouse.

Keywords

Oxidative stress; electrophilic stress; glutathione transferase; 4-hydroxynonenal; Nrf2; doxorubicin; cardiac function

Correspondence: Dr. Sharda P. Singh, Dept. of Pharmacology and Toxicology, University of Arkansas for Medical Sciences, 4301 West Markham Street, #638, Little Rock, AR 72205,U.S.A. SinghShardaP@uams.edu; Tel. +1 (501) 257-4806; FAX +1 (501) 257-6439.

Introduction

Oxidative stress and mitochondrial dysfunction, which can ultimately produce cell death through apoptosis or necrosis, have been implicated in the etiologies of many cardiovascular diseases (1–8). Oxidative stress usually arises from overproduction of reactive oxygen species (ROS) which in turn catalytically oxidize lipids and produce highly reactive products such as the α,β-unsaturated aldehydes: 4-HNE, acrolein, and malondialdehyde (reviewed in 9). 4-HNE is a highly reactive electrophile and forms protein and DNA adducts that are frequently detected in cardiac cells undergoing oxidative stress (10–12).

Besides its damaging effects, 4-HNE is an important signaling molecule at physiological levels (13) and participates in the activation of several key stress kinases (14–16) and the transcription factor Nrf2 (NF-E2-related factor 2) (reviewed in 17). Nrf2 binds *cis*-acting DNA sequences called antioxidant response elements (AREs; also called electrophile response elements, EpREs) to induce stress-responsive gene activity and specifically regulates genes responsible for countering oxidative and electrophilic stress. Nrf2 is bound in the cytosol by its repressor, the Kelch-like ECH associating protein 1 (Keap1) which functions as an adaptor for a Cullin 3 (Cul3)-based E3 ubiquitin ligase, a scaffold protein for the ubiquitination and degradation of Nrf2 (18). Keap1 regulates the degradation of Nrf2 in response to oxidants and electrophiles. Electrophiles, including 4-HNE, modify Keap1, causing it to dissociate from Nrf2 in the cytoplasm. Upon activation, Nrf2 translocates from the cytoplasm to the nucleus and binds to AREs, regulating selective gene transcription. The Keap1-Nrf2 pathway is involved in the regulation of most known genes responsible for ROS and 4-HNE disposition in different cell types, including cardiomyocytes (19–21).

Conjugation with glutathione by glutathione transferases (GSTs) is probably the predominant course of 4-HNE disposition in most vertebrate tissues (22). Previously, glutathione transferase alpha 4 (GSTA4-4) was shown to be abundantly expressed in protein extracts from whole mouse hearts (23) and to be localized within both the mitochondria and cytosol of mouse liver cells (24). A study of the human heart showed uniform staining of cardiomyocytes with a GSTA4-4 antibody (25).

To examine the regulation of electrophilic and oxidative stress *in vivo*, we generated a *Gsta4*-null mouse in the *129/sv* background. As expected, 4-HNE-conjugating activities are decreased in the tissues examined (23), including the heart. Only 23% of wild type (WT) 4-HNE-conjugating activity remains in the heart of *Gsta4*-null mice, clearly indicating that GSTA4-4 is the major GST disposing of 4-HNE in this critical tissue. Surprisingly, no cardiac pathology was detected in *Gsta4*-null mice.

In this study, we examined the biochemical basis for the cardiac phenotype of the *Gsta4*-null mouse. Despite highly reduced 4-HNE-conjugating activity in the hearts of *Gsta4*-null mice, we found no difference in cardiac 4-HNE levels between WT and null mice. We also observed a higher level of nuclear Nrf2 activity and increased expression of specific Nrf2 target genes in hearts of *Gsta4*-null mice. We hypothesized that a Nrf-2-driven compensatory mechanism might provide a responsive defense against further oxidative and electrophilic stress. Doxorubicin (DOX) is a very effective anti-tumor drug that is known to be cardiotoxic, primarily by inducing mitochondrial dysfunction and ensuing pathology (26–32). Specifically, as DOX trapped in cardiomyocyte mitochondria is transformed, high levels of superoxide and hydrogen peroxide are generated by redox cycling in mitochondria and the sarcoplasmic reticulum. Superoxide anion is also generated by DOX binding to endothelial nitric oxide synthase (eNOS). Both cardiomyocytes and endothelial cells are targets of DOX-induced apoptosis activated by increased ROS, oxidative stress and ensuing lipid peroxidation. DOX also reduces intracellular levels of antioxidants and inhibits cardiac

anti-oxidant enzymes. Hence, we challenged WT control and *Gsta4*-null mice with DOX: our findings suggest that *Gsta4*-null mice have an activated Nrf2-regulated defense mechanism in cardiac tissue that maintains steady-state levels of 4-HNE and may provide a form of preconditioning as a defense against DOX-induced cardiomyopathy involving redox changes.

Materials and Methods

Reagents and kits

The dimethylacetal ester of 4-hydroxy-2-transnonenal was synthesized according to Gree et al. (33), and Chandra and Srivastava (34) and stored at −80°C. Fresh 4-HNE was prepared before the assay by acid hydrolysis (pH 3.0) of the dimethylacetal ester. The Extract-N-Amp Tissue PCR Kit, butylated hydroxytoluene (BHT), NADH and doxorubicin were purchased from Sigma (St. Louis, MO). TRIzol Reagent, the Biotech LPO-586 kit, the QuantiTect Reverse Transcription Kit, the FastStart SYBR Green Master mix, the TransAM Nrf2 Kit, the Amplex Red Catalase Assay Kit (A22180) and the SOD Assay Kit-WST kit were purchased from Invitrogen/Life Technologies (Carlsbad, CA), Oxis International, (Portland, OR), Qiagen (Valencia, CA), Roche Diagnostics (Indianapolis, IN), Active Motif (Carlsbad, CA), Molecular Probes, Inc. (Eugene, OR) and Dojindo Molecular Technologies, Inc. (Rockville, MD), respectively. Primers for quantitative real-time PCR were synthesized by IDT (Coralville, IA, USA). A monoclonal antibody against cytoplasmic actin (catalog number sc-8432) was purchased from Santa Cruz Biotechnology (Santa Cruz, CA). All other reagents used in this study were of analytical grade.

Animals

The methods used to disrupt the *Gsta4* gene were described previously (23). The resulting *Gsta4*-null mice in the *129/sv* genetic background and matching WT mice in the same background were used for all experiments reported here. The genotype of mice with regard to the *mGsta4* gene was confirmed by PCR using tail biopsy samples (23). The work was performed in accordance with a protocol approved by the Central Arkansas Veterans Healthcare System Institutional Animal Care and Use Committee. Animals were housed in the Veterinary Medical Unit at the Central Arkansas Veterans Healthcare System in Little Rock, Arkansas.

Determination of 4-HNE levels

Tissues harvested from 16-week-old male WT and *Gsta4*-null mice were quick-frozen in liquid nitrogen using Wollenberger tongs (35) and stored at −75°C until use. 4-HNE levels in liver and heart samples from 16-week-old male WT and *Gsta4*-null mice were determined using the Biotech LPO-586 kit according to the manufacturer's protocol with slight modifications (36). A 20% (w/v) tissue homogenate was prepared in 20 mM Tris–HCl, pH 7.4, containing 5 mM BHT. The homogenates were centrifuged at 3,000 × g for 15 min, and 0.2 ml of the supernatants was used for each determination. To each sample, 650 μl of N-methyl-2-phenylindole and 150 μl of either 12 N HCl (for MDA determination) or 15.4 M methanesulfonic acid (for 4-HNE plus MDA determination) were added. The reaction mixtures were vortexed and incubated at 45°C for 60 min. After centrifugation at 15,000 × g for 10 min, the absorbance of the supernatants was determined at 586 nm.

Measurement of active Nrf2 binding

Hearts harvested from 16-week-old male WT and *Gsta4*-null mice were quick-frozen in liquid nitrogen using Wollenberger tongs and stored at −75°C. The level of active nuclear Nrf2 protein was determined by competitive ELISA, as previously described (37) using the

TransAM Nrf2 Kit according to the manufacturer's instructions. Briefly, nuclear extracts were prepared and contamination with cytosolic proteins was tested by western blotting for cytoplasmic actin using a monoclonal antibody against the actin C-terminus. Within the detection limits of the method, no cytosolic contamination was found in nuclei prepared from heart tissue (data not shown). Nuclear extracts (10 μg protein) were added to wells coated with an oligonucleotide containing the antioxidant response element (ARE) consensus sequence supplied by the TransAM Nrf2 Kit. Nrf2 specifically bound to the ARE was then revealed by adding anti-Nrf2 primary antibody. Detection of bound Nrf2 was achieved using a secondary antibody conjugated with horseradish peroxidase. Specificity of the reaction was confirmed by competition either with an ARE-containing oligonucleotide or a mutated, non-specific oligonucleotide supplied with the TransAM Nrf2 Kit. The amounts of active/bound Nrf2 were calculated after subtracting non-specific background values, determined by competition with the specific ARE oligonucleotide.

Determination of mRNA levels by reverse transcription real-time polymerase chain reaction

Total RNA was isolated from ventricular heart samples of 16-week-old male wild-type and *Gsta4*-null mice by the guanidinium thiocyanate method (38), using the TRIzol Reagent. Complementary DNA was prepared with the QuantiTect Reverse Transcription Kit according to the manufacturer's directions using the supplied mixture of oligo-dT and random primers. Reverse transcription real-time polymerase chain reactions (RT-qPCR) were performed on a DNA Engine Opticon 2 Detection System (MJ Research, Waltham, MA) with the FastStart SYBR Green Master mix in a total volume of 20 μL containing 0.3 μM gene-specific primers. The cycling protocol was an initial denaturation at 95°C for 10 minutes, followed by 40 cycles of 95°C for 15 seconds, 61°C for 30 seconds, and 72°C for 30 seconds. The ribosomal protein S3 (*RPS3*) transcript was used as a reference for normalization of *Akr1b7* mRNA levels and the *glyceraldehyde 3-phosphate dehydrogenase* (*Gapdh*) transcript for normalization of *Sod2*, *Cat,* and *Aldh2*. Primers were as follows: *Catalase* (Cat) forward: 5′-ACCAGGGCATCAAAAACTTG-3′ and *Cat* reverse: 5′-GCCCTGAAGCTTTTTGTCAG-3′ for a 134-bp product; *Superoxide dismutase* (*Sod2*) forward: 5′-GCGGTCGTGTAAACCTCAAT-3′, *Sod2* reverse: 5′-TAGGGCTCAGGTTTGTCCAG-3′ for a 100-bp product; *Aldehyde dehydrogenase 2* (*Aldh2*) forward: 5′-GCGGTCGTGTAAACCTCAAT-3′, *Aldh2* reverse: 5′-TAGGGCTCAGGTTTGTCCAG-3′ for a 70-bp product; Aldo-keto reductase 1b7 (*Akr1b7*) forward: 5′-GTGAAAGCTCTGGGCATCTC-3′, *Akr1b7* reverse: 5′-TGTCACAGACTTGGGATCA-3′ for a 103-bp product; 40S ribosomal protein S3 (*RPS3*) forward: 5′-TTACACCAACCAGGACAGAAATC-3′ and *RPS3* reverse: 5′-TGGACAACTGCGGTCAACTC-3′ for a 100-bp product; and *Gapdh* forward: 5′-CGTGTTCCTACCCCCAATGT-3′ and *Gapdh* reverse: 5′-CGTGTTCCTACCCCCAATGT-3′ for a 73-bp product. PCR products were positively identified by sequencing of each reaction product by the DNA Sequencing Core Facility at UAMS.

Anti-oxidant and anti-electrophile enzyme activities in the heart

Tissue homogenates were prepared from 16-week-old male WT and *Gsta4*-null mice euthanized by asphyxiation with carbon dioxide. A homogenate (10% w/v) of quick-frozen heart tissue was prepared with 20 mM potassium phosphate, pH 7.0, 1.4 mM 2-mercaptoethanol. Homogenates were clarified by centrifugation at 15,000 × g for 20 min at 4°C; and the supernatants were immediately used for activity measurements. Superoxide dismutase (SOD) activities was assayed using WST-1 (2-(4-iodophenyl)-3-(4-nitrophenyl)-5-(2,4-disulfo-phenyl)-2H-tetrazolium, monosodium salt) as a substrate producing a water-soluble formazan dye upon reduction with a superoxide anion. The rate of

WST-1 reduction by superoxide anion is linearly related to the xanthine oxidase activity and is inhibited by SOD. The IC_{50} (50% inhibitory concentration) of SOD was determined colorimetrically. SOD-2 activity was specifically measured by inhibition of SOD-1 and -3 activities, adding 1mM sodium cyanide in the reaction. The catalase assay was performed with the Amplex Red Kit using H_2O_2 as a substrate. In the assay, formation of resorufin was detected from reaction of any unreacted H_2O_2 and the Amplex Red reagent (N-acetyl-3,7-dihydroxyphenoxazine) in presence of horseradish peroxidase (HRP) (39). Measurements of activities of aldehyde dehydrogenase (ALDH), according to Manthey and Sladek (40) and Bunting et al. (41), and aldo-keto reductase 1 (AKR), according to Burczynski et al. (42), respectively, were measured using 4-HNE as a substrate.

Doxorubicin treatment and analysis

Eight WT and 8 *Gsta4*-null mice (aged 12–16 weeks) were administered intra-peritoneal injections of DOX for a total dose of 20 mg/kg (60 mg/m^2) in 4 weekly injections of 5 mg/kg (15 mg/m^2). Cardiac function of treated and control animals was assessed by transthoracic echocardiography using the Vevo 770 high-resolution *in vivo* micro-imaging system (VisualSonics, Toronto, Canada) with an RMV 707B Scanhead (center frequency 30 MHz, frequency band 15–45 MHz, and focal length 12.7 mm). Mice were anesthetized with and maintained under isoflurane during the procedure and positioned on a heated (37°C) platform that recorded both electrocardiogram and breathing pattern; an anal probe recorded body temperature. Echocardiographic parameters were obtained from two to three short axis M-mode recordings at the mid-left ventricular level of each mouse. Functional data on 8 WT and 8 *Gsta4*-null mice were obtained at 2 time points: day −1 (for baseline data) and day 21. DOX injections were administered 3 days after the first echocardiography, to allow the mice to recover, and then at 7-day intervals (day +2, +9, +16 and +23). All animals were monitored daily, recording their weight, physical appearance, and mortality.

Statistical analysis

Data were analyzed using Excel 2007 (Microsoft, Inc., Redmond, WA) and SAS versions 9.2 and 9.3 (the SAS Institute, Cary, NC). Differences in mRNA levels were analyzed by a two-factor ANOVA of two independent experiments. Genotypes were compared by two-tailed, unpaired *t* tests for differences in levels of 4-HNE, enzyme activities of catalase, SOD, ALDH, and AKR, and DNA-binding activity of Nrf2. Survival was analyzed using the log-rank test and Cox regression. Cardiac-function variables were analyzed via repeated-measures ANOVA with post-hoc contrasts to assess the group differences at each time point. *P*-values were statistically significant if less than 0.05, or marginally significant if between 0.05 and 0.10.

Results

4-HNE levels in the *Gsta4*-null mouse heart

Skeletal muscle, white adipose tissue, and liver had shown a significant elevation of 4-HNE levels in *Gsta4*-null mice, in the *129/sv* genetic background (23). Since 4-HNE levels in the heart were not examined previously, we compared 4-HNE levels in the heart and liver of *Gsta4*-null and WT mice. Surprisingly, we could detect no difference in 4-HNE levels in the *Gsta4*-null and WT hearts, in contrast to the liver, where the 4-HNE level was at least 2.5-fold higher in null mice (Fig. 1).

Higher levels of active Nrf2 in hearts of *Gsta4*-null mice

The similar levels of free 4-HNE in WT and *Gsta4*-null cardiac tissue suggested a possible compensatory mechanism, whereby, in the absence of 4-HNE-conjugating activity,

accumulating 4-HNE might activate the Keap1-Nrf2 pathway as a specific protective mechanism in the *Gsta4*-null heart. The transcription factor Nrf2 is known to regulate both ROS and 4-HNE metabolism by the activation of genes encoding anti-electrophilic and anti-oxidant enzymes in mammalian tissues, including the heart (20, 21, 43). Therefore, we compared the levels of Nrf2 DNA-binding activity in cardiac nuclear extracts from WT and *Gsta4*-null mice. We found a 2.15-fold increase ($p = 0.0002$) in active Nrf2 binding in the nuclear extracts of *Gsta4*-null mice as compared to WT mice (Fig. 2).

Nrf2 target gene expression

Enhanced Nrf2 signaling elicits upregulated expression of anti-oxidant enzymes and enzymes involved in 4-HNE disposition. In addition to conjugation by glutathione transferases, 4-HNE in the rodent heart is oxidized by aldehyde dehydrogenase or reduced by aldo-keto reductase (aldose reductase; (44). We examined mRNA levels of four Nrf2 target genes by quantitative reverse-transcription (qRT-PCR). In a comparison of WT and *Gsta4*-null mice, we found a 3-fold elevation in the mRNA level for *Sod2*, encoding the mitochondrial superoxide dismutase, a >2-fold increase in *catalase* mRNA level, and a minor increase in one of the aldo-keto reductase isozyme transcripts (*Akr1b7*) (Table 1). The *Aldehyde dehydrogenase 2* mRNA level, encoding a mitochondrial enzyme, decreased slightly in the *Gsta4*-null mouse heart (Table 1).

To determine if there is concomitant upregulation of anti-oxidant and, in particular, 4-HNE-metabolizing enzymes, we examined the enzyme activities of the corresponding Nrf2 target gene products. As shown in Fig. 3, we found significant increases in all the enzyme activities examined. Catalase activity was 12% higher, aldo-keto reductase (AKR) and aldehyde dehydrogenase (ALDH) were 30% and 29% higher, respectively, in *Gsta4*-null hearts as compared to those of WT mice. Total superoxide dismutase (SOD) activity was elevated 46%, while mitochondrial MnSOD (SOD2) was 42% higher and cytosolic & extracellular Cu-ZnSOD (SOD1 and 3) was 54% higher in *Gsta4*-null mice.

Effects of doxorubicin treatment on the *Gsta4*-null mouse

Although the exact mechanism of DOX-induced cardiotoxicity is complex, it is widely believed that DOX-generated reactive oxygen species (ROS) is the causative agent of cardiomyopathy (45). Since *Gsta4*-null mice exhibited no cardiac phenotype under normal conditions, we challenged them with DOX, which is known to produce oxidative stress, lipid peroxidation, and in particular, accumulation of 4-HNE in the rodent heart (26, 28, 46). Given the common DOX treatment schedules in clinical settings for human patients, we undertook a chronic treatment of *Gsta4*-null and WT mice with DOX. We found that WT mice were particularly sensitive to DOX, with only 2 animals surviving the 28-day duration of the experiment (Fig. 4). Survival analysis indicated that *Gsta4*-null mice had an 87% reduction in mortality from chronic DOX exposure as compared to WT mice (hazard ratio = 0.132; log-rank $p = 0.033$).

When baseline cardiac function was assessed by echocardiography (Echo 1 on day −1 of the DOX treatment schedule), untreated *Gsta4*-null mice (aged 12–16 weeks) exhibited no defect as compared to untreated WT mice (Table 2). However, after three DOX injections (15 mg/kg or 45 mg/m^2 total of DOX), only the hearts of WT mice revealed decreased cardiac function (Echo 2, Day 21): fractional shortening (FS) was lower as compared to both the WT baseline value ($p = 0.05$) and to FS of DOX-treated *Gsta4*-null mice on the same day ($p = 0.03$) (Table 2). Stroke volume also declined significantly in DOX-treated WT mice, but only mildly and insignificantly in hearts of *Gsta4*-null mice. A later time point could not be included in the cardiac function analysis, due to the sharp decline in survival of the WT mice.

Discussion

The murine mGSTA4-4, like its human homolog hGSTA4-4, has a very high catalytic efficiency for glutathione conjugation of the lipid peroxidation product 4-HNE (47) and is expressed at different levels in multiple tissues (23, 48), including the heart. We reported earlier that in *Gsta4*-null mice, in the *129/sv* genetic background, a decrease in 4-HNE-conjugating activity and an increase in 4-HNE levels were observed in the tissues examined (23, 36). The reduction in 4-HNE-conjugating activity in the hearts of *Gsta4*-null mice is particularly dramatic, with only 23% of residual conjugating activity remaining. This residual 4-HNE-conjugating activity could be largely due to Mu-class and/or other Alpha-class GSTs. With a major loss of 4-HNE-conjugating activity, higher levels of 4-HNE could be expected in the cardiac tissue of *Gsta4*-null mice, as seen in other tissues. However, the levels of 4-HNE in WT and *Gsta4*-null hearts were essentially the same (Fig. 1). This could be due to upregulation of either antioxidant enzymes that limit lipid peroxidation and thus 4-HNE formation, or of other detoxification enzymes that dispose of 4-HNE in cardiac cells (44). Furthermore, a higher level of 4-HNE in the wild-type *Gsta4*-null hearts, as compared to the liver (Fig. 1), may reflect especially high mitochondrial abundance in cardiomyocytes, subjecting them to increased oxidative stress (49) and resulting in higher steady-state levels of 4-HNE.

Expression of anti-oxidant and anti-electrophilic genes is largely controlled by the transcription factor Nrf2, known to induce stress-responsive gene expression, including those responsible for 4-HNE metabolism in the heart (44, 50, 51). As previously observed, both anti-oxidant and anti-electrophile reactions lower the concentration of 4-HNE and may constitute a negative feedback loop that stabilizes 4-HNE levels in the heart of *Gsta4*-null mice, possibly as a buffering mechanism to prevent 4-HNE concentration rising from protective to toxic levels (37). We recognize that other signaling pathways (such as JNK, NFKappa-B, PPAR alpha) are likely involved and undoubtedly also modulate the expression of genes involved in tissue protection. Yet, the hypothesis that Nrf2 plays a role in the induction of gene expression in cardiac cells of the *Gsta4*-null mouse is particularly attractive because of the documented ability of 4-HNE to activate Nrf2 (43).

In this study, we observed elevated Nrf2 binding activity in the hearts of untreated *Gsta*-null mice, while 4-HNE was maintained at normal physiological levels. Although the increase in active Nrf2 was statistically significant, its magnitude, approximately 2.15 folds (Fig. 2), was less than that reported for cells or animals treated with a variety of Nrf2 activators (52, 53). Typically, activation of Nrf2 is reported in terms of an increase in nuclear Nrf2 protein levels, determined by western blotting or by immunofluorescence. However, as all nuclear Nrf2 may not be active, antibody-based assays may overestimate Nrf2 activation.

To determine if the elevated Nrf2 binding activity in the *Gsta4*-null mouse heart results in increased cardiac Nrf2 signaling, we examined the products of four Nrf2 target genes (*Sod2, Cat, Aldh2,* and *Akr1b7*) whose expression is critical to oxidative and electrophilic stress responses. With one exception (*Aldh2*), increased mRNA levels were clearly associated with increases in enzyme activity levels, indicating that greater flux through the Nrf2 pathway has an impact on the cardiac phenotype of *Gsta4*-null mice. Furthermore and in particular, higher levels of mRNAs encoding catalase and SOD in the *Gsta4*-null mouse suggest that preventing the generation of 4-HNE by reducing oxidative stress might be more effective in maintaining physiological 4-HNE levels in the absence of the anti-electrophile enzyme, GSTA4-4.

In this study, we used DOX treatment to test *in vivo* the effects of elevated oxidative and electrophilic stress on the hearts of WT and *Gsta4*-null mice. DOX is a very effective cancer

treatment drug and is still widely used despite its dose-dependent and time-dependent cardiotoxicity which leads to increased ROS levels (primarily superoxide anion and hydrogen peroxide), lipid peroxidation and accumulation of 4-HNE in the heart (26, 28, 46). Animal and human studies indicate that DOX induces a form of dilated cardiomyopathy that is associated with interstitial inflammation, necrotic and apoptotic cell death, ventricular remodeling and fibrosis (32, 45). Depending on the severity of these pathological changes, cardiac function can be compromised and lead to heart failure. In *Gsta4*-null mice, we did not observe any significant change in two important measures of cardiac function: fractional shortening (FS) and stroke volume (SV) (Table 2). We did find a typical decrease in both FS and SV in WT mice that was not accompanied by increases in LVIDd or LVPWd as features of typical dilated cardiomyopathy. However, DOX-treated WT mice exhibited a commonly observed decrease in body weight (54, 55). Hence, from the survival analysis and two important cardiac function measures, we concluded that *Gsta4*-null mice were better able to resist DOX cardiotoxicity than WT mice.

Our results suggest that the higher nuclear Nrf2 binding activity in *Gsta4*-null mice, which helps to maintain 4-HNE at WT physiological levels by elevating at least four enzyme activities, may also contribute to preconditioning the heart in *Gsta4*-null mice and allow a stronger response to a DOX challenge. Recently, DOX was shown to significantly downregulate activity of the *Nrf2* gene as well as many of its target genes (56); the authors noted that deficiencies in these gene products could have implications for both DOX cardiotoxicity and its anti-tumor activity. Previous studies have shown that overexpression of mitochondrial SOD2 (MnSOD) (57, 58) or cytoplasmic catalase (59) can protect against DOX cardiomyopathy. Yet, many clinical trials have been unsuccessful in using exogenous antioxidants to confer cardioprotection during DOX treatment. However, cardiac preconditioning is a complex phenomenon that is usually associated with protection of the heart from ischemia-reperfusion injury and involves adaptive changes in signaling pathways (60). Various strategies have been adapted to attenuate DOX-induced cardiotoxicity by preconditioning animals and cells; these include exercise, various chemical treatments, thermal exposure, and brief ischemic episodes (61–67). For example, preconditioning of H9c2 cardiac cells by 4-HNE has been demonstrated to induce the alpha class GST isozyme, GSTA1-1 (68). In another study, cardiomyocytes preconditioned with a low concentration of 4-HNE (5μM) were resistant to higher concentrations of 4-HNE due to activation of Nrf2 and its target genes encoding protective enzymes (43). These studies and our *in vivo* findings suggest that the intracellular concentration of 4-HNE is critical for the induction of cardioprotective mechanisms. Preconditioning of the heart through use of the 4-HNE-activated Nrf2 pathway may be particularly successful by the upregulated expression of anti-oxidant and anti-electrophile enzymes as well as the synthesis of cellular antioxidants (such as glutathione). Additionally, since Nrf2-dependent signaling is thought to confer, in part, the protection imparted by dietary chemopreventive agents including flavones and polyphenols (69), our study supports approaches that enhance the efficacy of these chemopreventive agents to prevent cardiotoxicity when used as an adjuvant to cancer chemotherapy.

Acknowledgments

This research was supported by a grant from the National Institutes of Health, USA (AI046738 to S.P.S.) and a Pilot Study Grant (to H.B.) from the College of Medicine Research Council at the University of Arkansas for Medical Sciences. We thank Ludwika Zimniak (University of Arkansas for Medical Sciences) for her reading of the manuscript.

References

1. Heistad DD, Wakisaka Y, Miller J, Chu Y, Pena-Silva R. Novel aspects of oxidative stress in cardiovascular diseases. Circulation journal: official journal of the Japanese Circulation Society. 2009; 73:201–207. [PubMed: 19110503]
2. Ari E, Kaya Y, Demir H, Cebi A, Alp HH, Bakan E, Odabasi D, Keskin S. Oxidative DNA damage correlates with carotid artery atherosclerosis in hemodialysis patients. Hemodialysis international. 2011; 15:453–459. [PubMed: 22111813]
3. Fadel PJ, Farias M III, Gallagher KM, Wang Z, Thomas GD. Oxidative stress and enhanced sympathetic vasoconstriction in contracting muscles of nitrate-tolerant rats and humans. J Physiol (Lond). 2012; 590:395–407. [PubMed: 22106180]
4. Hollander JM, Baseler WA, Dabkowski ER. Proteomic remodeling of mitochondria in heart failure. Congestive Heart Failure. 2011; 17:262–268. [PubMed: 22103917]
5. Schlage WK, Westra JW, Gebel S, Catlett NL, Mathis C, Frushour BP, Hengstermann A, Van Hooser A, Poussin C, Wong B, Lietz M, Park J, Drubin D, Veljkovic E, Peitsch MC, Hoeng J, Deehan R. A computable cellular stress network model for non-diseased pulmonary and cardiovascular tissue. BMC Syst Biol. 2011; 5:168. [PubMed: 22011616]
6. Lee S, Park Y, Zuidema MY, Hannink M, Zhang C. Effects of interventions on oxidative stress and inflammation of cardiovascular diseases. World J Cardiol. 2011; 3:18–24. [PubMed: 21286214]
7. Le, Chen; Knowlton, AA. Mitochondrial Dynamics in Heart Failure. Congestive Heart Failure. 2011; 17:257–261. [PubMed: 22848903]
8. Dai DF, Rabinovitch PS, Ungvari Z. Mitochondria and cardiovascular aging. Circ Res. 2012; 110:1109–1124. [PubMed: 22499901]
9. Zimniak P. Relationship of electrophilic stress to aging. Free Radic Biol Med. 2011; 51:1087–1105. [PubMed: 21708248]
10. Churchill EN, Disatnik MH, Mochly-Rosen D. Time-dependent and ethanol-induced cardiac protection from ischemia mediated by mitochondrial translocation of varepsilonPKC and activation of aldehyde dehydrogenase 2. J Mol Cell Cardiol. 2009; 46:278–284. [PubMed: 18983847]
11. Dhiman M, Zago MP, Nunez S, Amoroso A, Rementeria H, Dousset P, Nunez Burgos F, Garg NJ. Cardiac-oxidized antigens are targets of immune recognition by antibodies and potential molecular determinants in chagas disease pathogenesis. PloS one. 2012; 7:e28449. [PubMed: 22238578]
12. Hayashida K, Sano M, Kamimura N, Yokota T, Suzuki M, Maekawa Y, Kawamura A, Abe T, Ohta S, Fukuda K, Hori S. H(2) gas improves functional outcome after cardiac arrest to an extent comparable to therapeutic hypothermia in a rat model. J Am Heart Assoc. 2012; 1:e003459. [PubMed: 23316300]
13. Awasthi YC, Sharma R, Sharma A, Yadav S, Singhal SS, Chaudhary P, Awasthi S. Self-regulatory role of 4-hydroxynonenal in signaling for stress-induced programmed cell death. Free Radic Biol Med. 2008; 45:111–118. [PubMed: 18456001]
14. Uchida K, Shiraishi M, Naito Y, Torii Y, Nakamura Y, Osawa T. Activation of stress signaling pathways by the end product of lipid peroxidation - 4-hydroxy-2-nonenal is a potential inducer of intracellular peroxide production. J Biol Chem. 1999; 274:2234–2242. [PubMed: 9890986]
15. Ma H, Guo R, Yu L, Zhang Y, Ren J. Aldehyde dehydrogenase 2 (ALDH2) rescues myocardial ischaemia/reperfusion injury: role of autophagy paradox and toxic aldehyde. Eur Heart J. 2011; 32:1025–1038. [PubMed: 20705694]
16. Pajaud J, Kumar S, Rauch C, Morel F, Aninat C. Regulation of signal transduction by glutathione transferases. Int J Hepatol. 2012; 2012:137676. [PubMed: 23094162]
17. Kansanen E, Jyrkkanen HK, Levonen AL. Activation of stress signaling pathways by electrophilic oxidized and nitrated lipids. Free Radic Biol Med. 2012; 52:973–982. [PubMed: 22198184]
18. Zhang DD, Lo SC, Cross JV, Templeton DJ, Hannink M. Keap1 is a redox-regulated substrate adaptor protein for a Cul3-dependent ubiquitin ligase complex. Mol Cell Biol. 2004; 24:10941–10953. [PubMed: 15572695]
19. Taylor RC, Acquaah-Mensah G, Singhal M, Malhotra D, Biswal S. Network inference algorithms elucidate Nrf2 regulation of mouse lung oxidative stress. PLoS Comp Biol. 2008; 4:e1000166.

20. Zhu H, Jia Z, Misra BR, Zhang L, Cao Z, Yamamoto M, Trush MA, Misra HP, Li Y. Nuclear factor E2-related factor 2-dependent myocardiac cytoprotection against oxidative and electrophilic stress. Cardiovasc Toxicol. 2008; 8:71–85. [PubMed: 18463988]
21. Aleksunes LM, Klaassen CD. Coordinated regulation of hepatic phase I and II drug-metabolizing genes and transporters using AhR-, CAR-, PXR-, PPARalpha-, and Nrf2-null mice. Drug metabolism and disposition: the biological fate of chemicals. 2012; 40:1366–1379. [PubMed: 22496397]
22. Balogh LM, Atkins WM. Interactions of glutathione transferases with 4-hydroxynonenal. Drug Metab Rev. 2011; 43:165–178. [PubMed: 21401344]
23. Engle MR, Singh SP, Czernik PJ, Gaddy D, Montague DC, Ceci JD, Yang Y, Awasthi S, Awasthi YC, Zimniak P. Physiological role of mGSTA4-4, a glutathione S-transferase metabolizing 4-hydroxynonenal: generation and analysis of mGsta4 null mouse. Toxicol Appl Pharmacol. 2004; 194:296–308. [PubMed: 14761685]
24. Raza H, Robin MA, Fang JK, Avadhani NG. Multiple isoforms of mitochondrial glutathione S-transferases and their differential induction under oxidative stress. Biochem J. 2002; 366:45–55. [PubMed: 12020353]
25. Desmots F, Rissel M, Loyer P, Turlin B, Guillouzo A. Immunohistological analysis of glutathione transferase A4 distribution in several human tissues using a specific polyclonal antibody. J Histochem Cytochem. 2001; 49:1573–1580. [PubMed: 11724905]
26. Chaiswing L, Cole MP, St Clair DK, Ittarat W, Szweda LI, Oberley TD. Oxidative damage precedes nitrative damage in adriamycin-induced cardiac mitochondrial injury. Toxicol Pathol. 2004; 32:536–547. [PubMed: 15605432]
27. Menna P, Salvatorelli E, Minotti G. Doxorubicin degradation in cardiomyocytes. J Pharmacol Exp Ther. 2007; 322:408–419. [PubMed: 17468298]
28. Jungsuwadee P, Nithipongvanitch R, Chen Y, Oberley TD, Butterfield DA, St Clair DK, Vore M. Mrp1 localization and function in cardiac mitochondria after doxorubicin. Mol Pharmacol. 2009; 75:1117–1126. [PubMed: 19233900]
29. Zhao Y, McLaughlin D, Robinson E, Harvey AP, Hookham MB, Shah AM, McDermott BJ, Grieve DJ. Nox2 NADPH oxidase promotes pathologic cardiac remodeling associated with Doxorubicin chemotherapy. Cancer Res. 2010; 70:9287–9297. [PubMed: 20884632]
30. Richard C, Ghibu S, Delemasure-Chalumeau S, Guilland JC, Des Rosiers C, Zeller M, Cottin Y, Rochette L, Vergely C. Oxidative stress and myocardial gene alterations associated with Doxorubicin-induced cardiotoxicity in rats persist for 2 months after treatment cessation. J Pharmacol Exp Ther. 2011; 339:807–814. [PubMed: 21934029]
31. Xi L, Zhu SG, Das A, Chen Q, Durrant D, Hobbs DC, Lesnefsky EJ, Kukreja RC. Dietary inorganic nitrate alleviates doxorubicin cardiotoxicity: mechanisms and implications. Nitric Oxide. 2012; 26:274–284. [PubMed: 22484629]
32. Octavia Y, Tocchetti CG, Gabrielson KL, Janssens S, Crijns HJ, Moens AL. Doxorubicin-induced cardiomyopathy: from molecular mechanisms to therapeutic strategies. J Mol Cell Cardiol. 2012; 52:1213–1225. [PubMed: 22465037]
33. Grée R, Tourbah H, Carrié R. Fumaraldehyde monodimethyl acetal: An easily accessible and versatile intermediate. Tetrahedron Lett. 1986; 27:4983–4986.
34. Chandra A, Srivastava SK. A synthesis of 4-hydroxy-2-trans-nonenal and 4-(3H) 4-hydroxy-2-trans-nonenal. Lipids. 1997; 32:779–782. [PubMed: 9252968]
35. Wollenberger A, Ristau O, Schoffa G. A simple technic for extremely rapid freezing of large pieces of tissue. Pflugers Arch Gesamte Physiol Menschen Tiere. 1960; 270:399–412.
36. Singh SP, Niemczyk M, Saini D, Awasthi YC, Zimniak L, Zimniak P. Role of the electrophilic lipid peroxidation product 4-hydroxynonenal in the development and maintenance of obesity in mice. Biochemistry (Mosc). 2008; 47:3900–3911.
37. Singh SP, Niemczyk M, Saini D, Sadovov V, Zimniak L, Zimniak P. Disruption of the mGsta4 gene increases life span of C57BL mice. J Gerontol A Biol Sci Med Sci. 2010; 65:14–23. [PubMed: 19880816]
38. Chomczynski P, Sacchi N. Single-step method of RNA isolation by acid guanidinium thiocyanate-phenol-chloroform extraction. Anal Biochem. 1987; 162:156–159. [PubMed: 2440339]

39. Mohanty JG, Jaffe JS, Schulman ES, Raible DG. A highly sensitive fluorescent micro-assay of H2O2 release from activated human leukocytes using a dihydroxyphenoxazine derivative. J Immunol Methods. 1997; 202:133–141. [PubMed: 9107302]
40. Manthey CL, Sladek NE. Kinetic characterization of the catalysis of “activated” cyclophosphamide (4-hydroxycyclophosphamide/aldophosphamide) oxidation to carboxyphosphamide by mouse hepatic aldehyde dehydrogenases. Biochem Pharmacol. 1988; 37:2781–2790. [PubMed: 3395357]
41. Bunting KD, Lindahl R, Townsend AJ. Oxazaphosphorine-specific resistance in human MCF-7 breast carcinoma cell lines expressing transfected rat class 3 aldehyde dehydrogenase. J Biol Chem. 1994; 269:23197–23203. [PubMed: 8083225]
42. Burczynski ME, Sridhar GR, Palackal NT, Penning TM. The reactive oxygen species--and Michael acceptor-inducible human aldo-keto reductase AKR1C1 reduces the alpha,beta-unsaturated aldehyde 4-hydroxy-2-nonenal to 1,4-dihydroxy-2-nonene. J Biol Chem. 2001; 276:2890–2897. [PubMed: 11060293]
43. Zhang Y, Sano M, Shinmura K, Tamaki K, Katsumata Y, Matsuhashi T, Morizane S, Ito H, Hishiki T, Endo J, Zhou H, Yuasa S, Kaneda R, Suematsu M, Fukuda K. 4-hydroxy-2-nonenal protects against cardiac ischemia-reperfusion injury via the Nrf2-dependent pathway. J Mol Cell Cardiol. 2010; 49:576–586. [PubMed: 20685357]
44. Srivastava S, Chandra A, Wang LF, Seifert WE Jr, DaGue BB, Ansari NH, Srivastava SK, Bhatnagar A. Metabolism of the lipid peroxidation product, 4-hydroxy-trans-2-nonenal, in isolated perfused rat heart. J Biol Chem. 1998; 273:10893–10900. [PubMed: 9556565]
45. Sterba M, Popelova O, Vavrova A, Jirkovsky E, Kovarikova P, Gersl V, Simunek T. Oxidative stress, redox signaling, and metal chelation in anthracycline cardiotoxicity and pharmacological cardioprotection. Antioxid Redox Signal. 2013; 18:899–929. [PubMed: 22794198]
46. Luo X, Evrovsky Y, Cole D, Trines J, Benson LN, Lehotay DC. Doxorubicin-induced acute changes in cytotoxic aldehydes, antioxidant status and cardiac function in the rat. Biochim Biophys Acta. 1997; 1360:45–52. [PubMed: 9061039]
47. Zimniak P, Singhal SS, Srivastava SK, Awasthi S, Sharma R, Hayden JB, Awasthi YC. Estimation of genomic complexity, heterologous expression, and enzymatic characterization of mouse glutathione S-transferase mGSTA4-4 (GST 5.7). J Biol Chem. 1994; 269:992–1000. [PubMed: 7904605]
48. Knight TR, Choudhuri S, Klaassen CD. Constitutive mRNA expression of various glutathione S-transferase isoforms in different tissues of mice. Toxicol Sci. 2007; 100:513–524. [PubMed: 17890767]
49. Prosser BL, Ward CW, Lederer WJ. X-ROS signaling: rapid mechano-chemo transduction in heart. Science. 2011; 333:1440–1445. [PubMed: 21903813]
50. Thimmulappa RK, Mai KH, Srisuma S, Kensler TW, Yamamoto M, Biswal S. Identification of Nrf2-regulated genes induced by the chemopreventive agent sulforaphane by oligonucleotide microarray. Cancer Res. 2002; 62:5196–5203. [PubMed: 12234984]
51. Lou H, Du S, Ji Q, Stolz A. Induction of AKR1C2 by phase II inducers: identification of a distal consensus antioxidant response element regulated by NRF2. Mol Pharmacol. 2006; 69:1662–1672. [PubMed: 16478829]
52. Goldring CE, Kitteringham NR, Elsby R, Randle LE, Clement YN, Williams DP, McMahon M, Hayes JD, Itoh K, Yamamoto M, Park BK. Activation of hepatic Nrf2 in vivo by acetaminophen in CD-1 mice. Hepatology. 2004; 39:1267–1276. [PubMed: 15122755]
53. Li Y, Paonessa JD, Zhang Y. Mechanism of chemical activation of Nrf2. PloS one. 2012; 7:e35122. [PubMed: 22558124]
54. Doroshow JH, Locker GY, Ifrim I, Myers CE. Prevention of doxorubicin cardiac toxicity in the mouse by N-acetylcysteine. J Clin Invest. 1981; 68:1053–1064. [PubMed: 7287901]
55. Lu M, Merali S, Gordon R, Jiang J, Li Y, Mandeli J, Duan X, Fallon J, Holland JF. Prevention of Doxorubicin cardiopathic changes by a benzyl styryl sulfone in mice. Genes Cancer. 2011; 2:985–992. [PubMed: 22701764]
56. Todorova VK, Beggs ML, Delongchamp RR, Dhakal I, Makhoul I, Wei JY, Klimberg VS. Transcriptome profiling of peripheral blood cells identifies potential biomarkers for Doxorubicin cardiotoxicity in a rat model. PloS one. 2012; 7:e48398. [PubMed: 23209553]

57. Yen HC, Oberley TD, Gairola CG, Szweda LI, St Clair DK. Manganese superoxide dismutase protects mitochondrial complex I against adriamycin-induced cardiomyopathy in transgenic mice. Arch Biochem Biophys. 1999; 362:59–66. [PubMed: 9917329]
58. Cole MP, Chaiswing L, Oberley TD, Edelmann SE, Piascik MT, Lin SM, Kiningham KK, St Clair DK. The protective roles of nitric oxide and superoxide dismutase in adriamycin-induced cardiotoxicity. Cardiovasc Res. 2006; 69:186–197. [PubMed: 16157314]
59. Kang YJ, Sun X, Chen Y, Zhou Z. Inhibition of doxorubicin chronic toxicity in catalase-overexpressing transgenic mouse hearts. Chem Res Toxicol. 2002; 15:1–6. [PubMed: 11800590]
60. Bell RM, Yellon DM. Conditioning the whole heart--not just the cardiomyocyte. J Mol Cell Cardiol. 2012; 53:24–32. [PubMed: 22521304]
61. Ito H, Shimojo T, Fujisaki H, Tamamori M, Ishiyama S, Adachi S, Abe S, Marumo F, Hiroe M. Thermal preconditioning protects rat cardiac muscle cells from doxorubicin-induced apoptosis. Life Sci. 1999; 64:755–761. [PubMed: 10075108]
62. Liu X, Chen Z, Chua CC, Ma YS, Youngberg GA, Hamdy R, Chua BH. Melatonin as an effective protector against doxorubicin-induced cardiotoxicity. American Journal of Physiology: Heart and Circulatory Physiology. 2002; 283:H254–263. [PubMed: 12063298]
63. Hofmann PA, Israel M, Koseki Y, Laskin J, Gray J, Janik A, Sweatman TW, Lothstein L. N-Benzyladriamycin-14-valerate (AD 198): a non-cardiotoxic anthracycline that is cardioprotective through PKC-epsilon activation. J Pharmacol Exp Ther. 2007; 323:658–664. [PubMed: 17693586]
64. Kim KH, Oudit GY, Backx PH. Erythropoietin protects against doxorubicin-induced cardiomyopathy via a phosphatidylinositol 3-kinase-dependent pathway. J Pharmacol Exp Ther. 2008; 324:160–169. [PubMed: 17928571]
65. Calvert JW, Coetzee WA, Lefer DJ. Novel insights into hydrogen sulfide--mediated cytoprotection. Antioxid Redox Signal. 2010; 12:1203–1217. [PubMed: 19769484]
66. Hydock DS, Lien CY, Jensen BT, Schneider CM, Hayward R. Exercise preconditioning provides long-term protection against early chronic doxorubicin cardiotoxicity. Integrative Cancer Therapies. 2011; 10:47–57. [PubMed: 21382960]
67. Muthusamy VR, Kannan S, Sadhaasivam K, Gounder SS, Davidson CJ, Boeheme C, Hoidal JR, Wang L, Rajasekaran NS. Acute exercise stress activates Nrf2/ARE signaling and promotes antioxidant mechanisms in the myocardium. Free Radic Biol Med. 2012; 52:366–376. [PubMed: 22051043]
68. Zhu H, Zhang L, Xi X, Zweier JL, Li Y. 4-Hydroxy-2-nonenal upregulates endogenous antioxidants and phase 2 enzymes in rat H9c2 myocardiac cells: protection against overt oxidative and electrophilic injury. Free Radic Res. 2006; 40:875–884. [PubMed: 17015266]
69. Giudice A, Arra C, Turco MC. Review of molecular mechanisms involved in the activation of the Nrf2-ARE signaling pathway by chemopreventive agents. Methods Mol Biol. 2010; 647:37–74. [PubMed: 20694660]

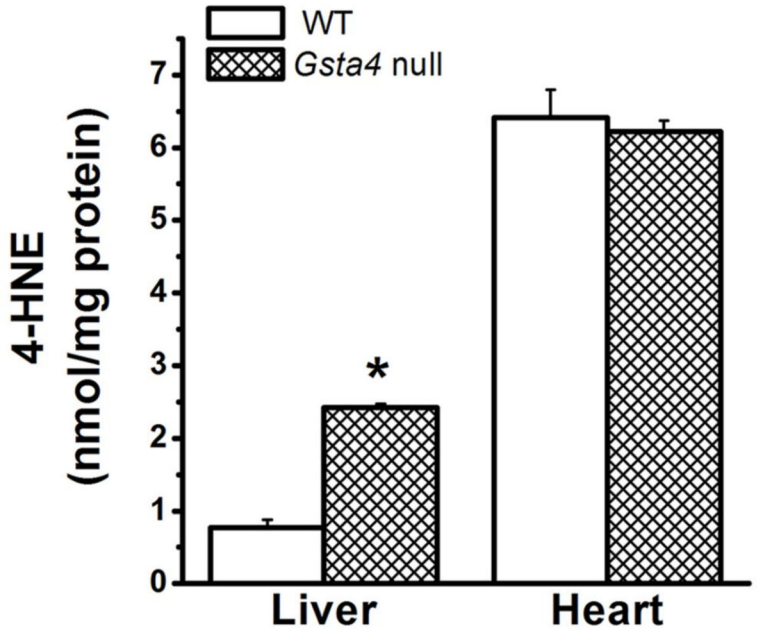

Fig. 1.

No difference in cardiac 4-HNE levels between wild-type and *Gsta4*-null mice. 4-HNE levels were determined, as previously reported (23), in liver and cardiac tissue samples from 16-week-old male mice. The difference between the null and wild-type mice was only significant for the liver (*, $p = 2\times10^{-4}$, n=4).

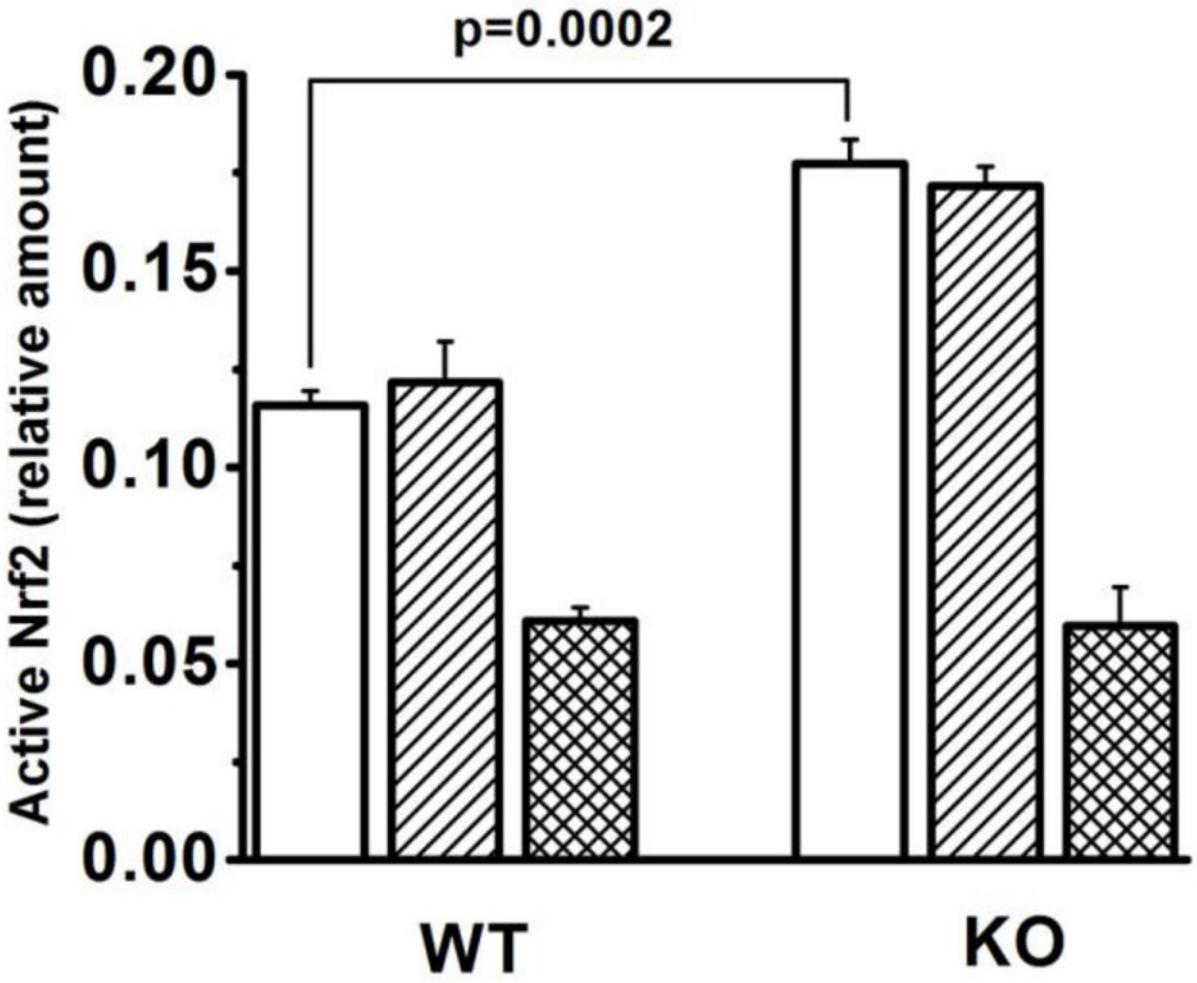

Fig. 2.

Different levels of active nuclear Nrf2 in hearts of wild-type and *Gsta4*-null mice. Active Nrf2 binding was measured in nuclear extracts from whole hearts of male WT and *Gsta4*-null mice (16 weeks of age). Open bars: nuclear extract; hatched bars: nuclear extract + mutated probe; cross-hatched bars: nuclear extract + competitive ARE probe. Each bar represents the mean ± SD (n=4); statistical significance, as shown, was evaluated by the *t*-test.

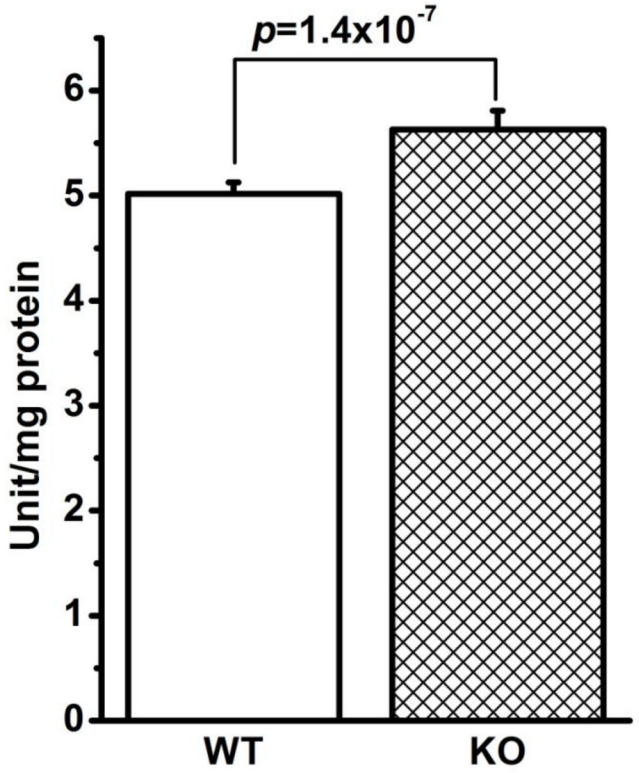

Fig. 3A.

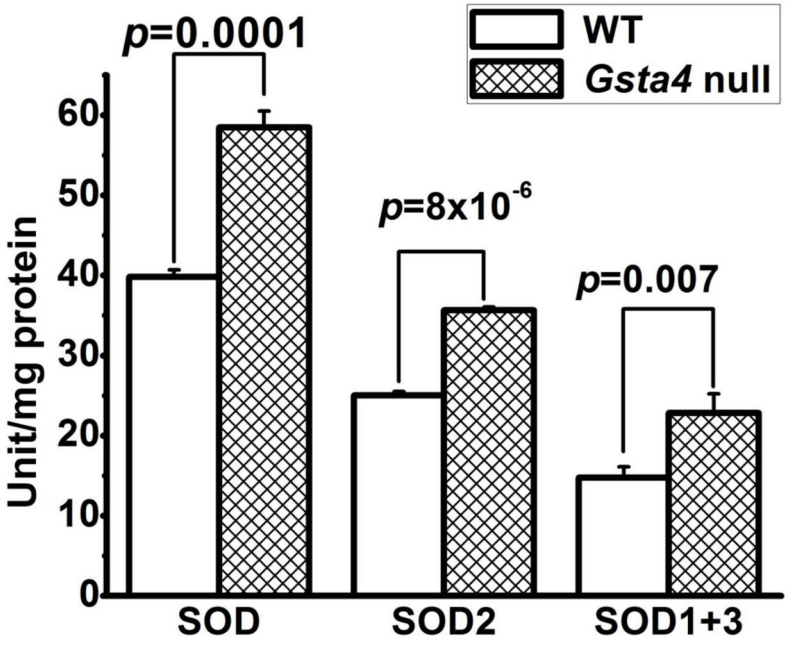

Fig. 3B.

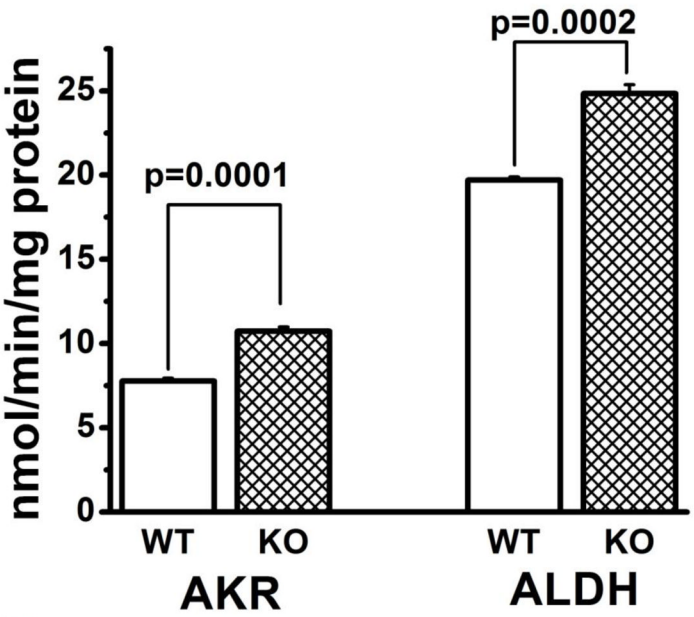

Fig. 3C.

Fig. 3.

Anti-oxidant and anti-electrophile activities in WT and *Gsta4 null* (KO) mice. All enzyme activities were measured in heart extracts of 16-week old male mice as described in the Methods. Each bar represents the mean ± SD (n=4); statistical significance, as shown, was evaluated by a *t*-test. **(A)** Catalase activity was assayed using H_2O_2 as a substrate. **(B)** SOD enzyme activities were determined using WST1 (see Methods) as a substrate. **(C)** AKR and ALDH activities were measured using 4-HNE as a substrate.

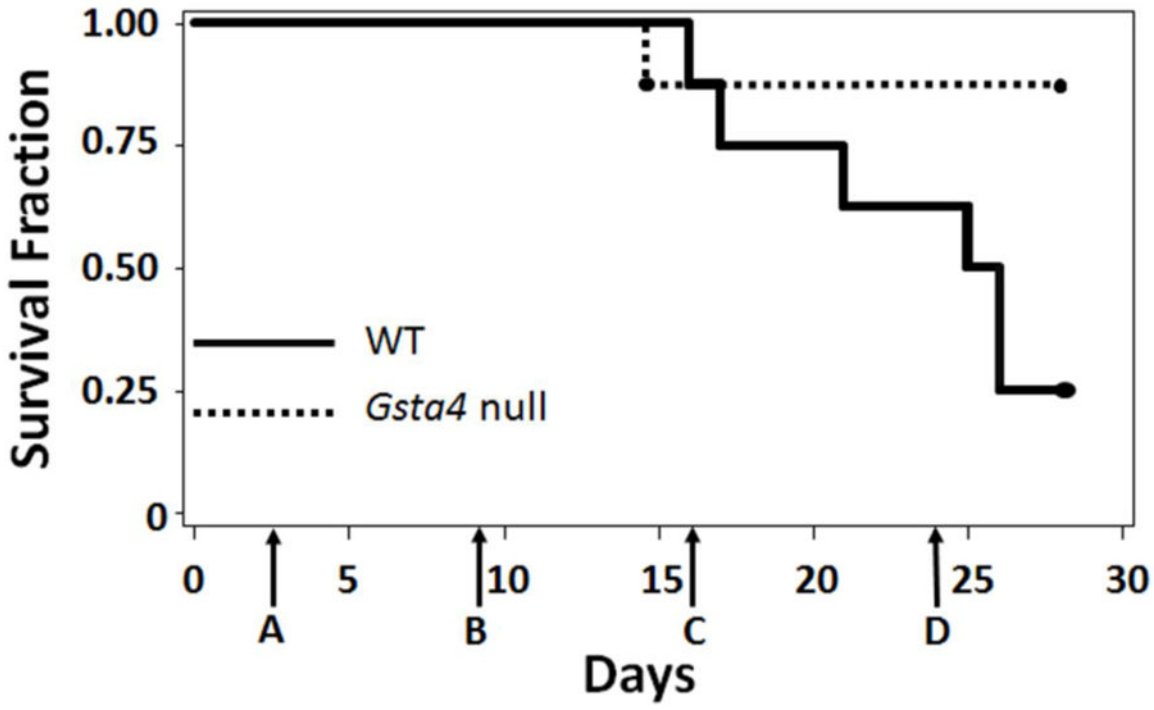

Fig. 4.

Survival of *Gsta4*-null and WT mice treated with DOX. 8 WT and 8 *Gsta4*-null mice (male, 12–16 weeks of age) were injected weekly (indicated by arrows) with 5 mg/kg DOX for 4 weeks. Survival, analyzed using the log-rank test and Cox regression, indicated that *Gsta4*-null mice had a significant reduction in mortality (hazard ratio = 0.132; log-rank $p = 0.033$).

Table 1

Upregulation of selected Nrf2 target genes in the *Gsta4*-null mouse. Transcript levels of genes encoding different oxidative or electrophilic stress response enzymes were measured by qRT-PCR (as described in Materials and Methods).

Gene	Fold Change, KO/WT	*p*
Akr1b7	**1.6** (1.3–2.0)	0.054
Aldh2	**0.7** (0.6–0.8)	0.020
Cat	**2.4** (1.9–3.0)	0.005
Sod2	**3.1** (2.0–4.8)	0.026

The range of fold changes is indicated in parentheses. Significance is indicated by the *p* value.

Table 2

Cardiac function parameters in doxorubicin-treated WT and *Gsta4* KO mice.

Parameter	Wild-type		*Gsta4* KO	
	Echo 1 (n=8)	**Echo 2 (n=5)**	**Echo 1 (n=8)**	**Echo 2 (n=7)**
FS (%)	35.08±6.11	29.24±4.12 *	34.13±7.10	34.00±2.74
SV (μl)	41.88±7.00	32.13±3.14 ¶	38.27±6.51	35.73±2.89
LVIDd (mm)	3.80±0.42	3.65±0.3	3.73±0.13	3.64±0.18
LVPWd (mm)	0.86±0.12	0.89±0.13	0.85±0.13	0.96±0.18
HR (bpm)	338±45	284±28	334±36	287±62
LVmass (mg)	96.0±20.3	92.6±3.4	103.4±11.7	104.5±17.0
BW (g)	25.9±2.3	22.6±0.9 #	26.9±2.6	26.4±2.0
LVmass/BW (mg/g)	3.7±0.5	4.1±0.1	3.9±0.4	4.0±0.8

Echo 1 was performed two days before the first DOX injection; Echo 2 was done on day 21 after a cumulative dose of 15 mg/kg (45 mg/m^2). FS, fractional shortening; SV, stroke volume; LVIDd, left ventricle internal diameter at the end of diastole; LVPWd, left ventricle posterior wall thickness at end of diastole; HR, heart rate; LVmass, left ventricle mass; BW, body weight; LVmass/BW, left ventricle mass/body weight ratio. Table values are means±standard deviation.

* $p<0.05$ versus WT Echo 1 or KO Echo 2;

¶ $p<0.002$ versus WT Echo 1;

\# $p<0.01$ versus WT Echo 1 or KO Echo 2 (by repeated-measures ANOVA).